Proceedings of the 2012 24th International Symposium on Power Semiconductor Devices and ICs
3-7 June 2012 - Bruges, Belgium

Breakdown Voltage Enhancement for Power AlGaN/GaN HEMTs with Air-bridge Field Plate

G. Xie [1,2], E. Xu [1], J. Lee [1], N. Hashemi [1], W. T. Ng [1]
[1] University of Toronto
The Edward S. Rogers Sr. Department of Electrical and Computer Engineering
Toronto, Ontario, Canada
E-mail: xielyz@vrg.utoronto.ca
E-mail: ngwt@vrg.utoronto.ca

B. Zhang [2]
[2] University of Electronic Science and Technology of China
State Key Laboratory of Electronic Thin Films and Integrated Devices
Chengdu, Sichuan, China
E-mail: zhangbo@uestc.edu.cn

F. Y. Fu [3]
[3] Crosslight software Inc.
Burnaby, BC, Canada
E-mail: fred@crosslight.com

***Abstract*— An AlGaN/GaN high-electron mobility transistor (HEMT) with a novel source-connected Air-bridge Field Plate (AFP) is simulated, optimized and experimentally verified. The device features a metal field plate that jumps from the source over the gate region and lands between gate and drain. The fabrication process is based on a commercially available RF GaN on SiC technology. Device characteristics for this work were optimized via layout changes only. An extensive analysis on the surface electrical field distribution was used to study the effect of varying AFP dimension. Simulation results indicated a breakdown voltage of 425 V for the AFP device can be achieved at V_{GS} = −5 V. The gate to drain distance is 6 µm and the gate length is 0.8 µm. The fabricated results for AFP device are in relatively good agreement with the simulation results and exhibit improvement in forward blocking voltage of 375 V at V_{GS} = −5 V. This is a factor of 3× improvement when compared to the best device that can be fabricated using conventional field plate (FP) for this particular process. The measured specific on-resistance for the device with the proposed AFP is 0.58 mΩ·cm^2 at V_{GS} = 0 V, which compares favorably with 0.79 mΩ·cm^2 for the device with a conventional FP.**

Keywords-GaN Power Devices; AlGaN/GaN HEMTs, Air-bridge Field Plate; Breakdown Voltage; Electric Field; Gate to Source capacitance

I. INTRODUCTION

AlGaN/GaN high electron mobility transistors (HEMTs) have been popular for power electronics and RF applications due to their high breakdown field, high mobility 2D electron gas (2-DEG), high saturation velocity and low intrinsic carrier density [1-4]. Recent work has placed emphasis on improving the OFF-state blocking capability without introducing process complexity and parasitic. Field Plate (FP) structures have been shown to be effective in enhancing the breakdown voltage and reducing C_{gd} for silicon power devices [5-6]. In addition, FP can improve device reliability and suppress current collapse from occurring in AlGaN/GaN HEMTs [7]. However, for commercially RF process, only limited breakdown voltage improvement can be obtained with conventional FP structures due to undesirable thickness of the SiN passivation (e.g. 150 nm). Base on such thin SiN passivation thickness, FP is less effective. K. S. Boutros *et al.* [8] fabricated a HEMT with source field plate length of 0.7µm can only provide a breakdown voltage of 200 V.

In addition, the source-connected FP structure reduces C_{gd}, but at the cost of a slight increase in C_{gs}, especially for long gate length [9].

In this paper, a novel source-connected Air-bridge Field Plate (AFP) is introduced to achieve high breakdown voltage even with very thin SiN passivation of 150 nm on a RF process. HEMT devices with conventional source-connected FP over the same thickness of SiN layer were also fabricated for comparison purpose. Fabrication results indicated that the proposed air-bridge devices exhibit a 3× improvement in OFF-state breakdown voltage when compared to devices with conventional FP. Crosslight-APSYS [10] numerical analysis was carried out to help analyze the detailed electrical characteristics. Simulation results showed good agreement with the fabrication results.

II. DEVICE STRUCTURE AND SIMULATION MODELS

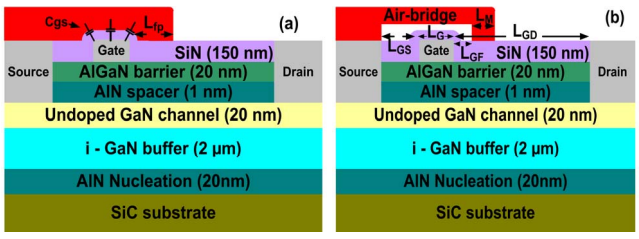

Fig.1 (a) Schematic cross-section of AlGaN/GaN HEMT with conventional field plate, where L_{FP} is the field plate length. (b) with Novel Air−bridge Field Plate (AFP), where L_{GS}, L_G, L_{GF}, L_M and L_{GD} are the gate–source distance, gate length, gate to air bridge field plate distance, air bridge footprint width and gate–drain distance (drift region), respectively.

Device with AFP and conventional FP are as shown in Fig. 1. The epitaxial layer structure consists of an unintentionally doped AlGaN barrier layer (20 nm)/i-AlN spacing layer (1 nm)/i-GaN channel layer (200 nm)/C-doped insulating layer (2 µm)/ AlN nucleation layer (20 nm). Al mole fraction in the AlGaN layer was 0.28. The thickness of the SiN passivation layer is 150 nm. A sheet carrier density of 1.1×10^{13} cm^{-2} caused by the piezoelectric and polarization dipole was modeled along the upper side of the AlGaN/GaN interface to define the 2-DEG sheet carrier concentration. According to Chynoweth [11] impact ionization model and Monte Carlo simulation of the impact ionization in Wurtzite GaN[12], electron ionization rates and hole ionization rates can be calculated to be 2.6×10^{8} cm^{-1} and 4.98×10^{6} cm^{-1}, respectively. Traps with a maximum concentration of 1×10^{14} cm^{-3} and a relative energy level of 1.1 eV were also assigned to model the semi-insulating substrate to suppress parasitic conduction. Electron mobility of 1800 cm^2 V^{-1} S^{-1} was used in the simulation. Other device parameter values employed for simulation are as shown in Table 1.

TABLE I
MATERIAL PARAMETERS FOR SIMULATION

Parameters	AlGaN	GaN
Bandgap (eV)	4.15	3.47
Electron mobility ($cm^2V^{-1}S^{-1}$)	550	1100
Electron saturation velocity (cms^{-1})	1.5×10^7	2.1×10^7
Dielectric constant	9.6	9.5
Critical electric field (MV/cm)	5.5	3.3

III. Simulation Results and Analysis

The simulated HEMT with air-bridge FP features a source to gate access length, L_{GS} = 1.1µm, a gate to drain spacing, L_{GD} = 6 µm, and a gate length, L_G = 0.8 µm. HEMTs without FP, with conventional FP and with air-bridge FP were simulated with the same physical dimensions.

Breakdown voltages as a function of FP length and air-bridge FP length are as shown in Fig. 2. Conventional HEMT without FP shows 60 V of breakdown voltage. Breakdown voltage increases from 60 V without FP to 240 V maximum with conventional FP length of 1 µm with no further increase after this point. Conventional FP HEMTs show limited breakdown voltage improvement due to relative thin SiN passivation. Premature breakdown occurs near the FP edge.

The simulated breakdown voltages (V_{BR}) as a function of L_M with different L_{GF} are also as shown in Fig. 2 (b). Air-bridge FP HEMTs exhibit remarkable improvement in breakdown voltage. Breakdown voltage reaches as high as 450V with L_M = 2 µm, L_{GF} = 0.5 µm, which is around 2 times higher than that of conventional FP technique. The low dielectric constant of air can better modulate the surface electric distribution shown in Fig.3 (a). As illustrated in Fig. 3 (a), the surface electric field distribution along the AlGaN/GaN interface for the AFP structure exhibits lower electric field strength near both the drain side gate edge and FP edge. This clearly shows

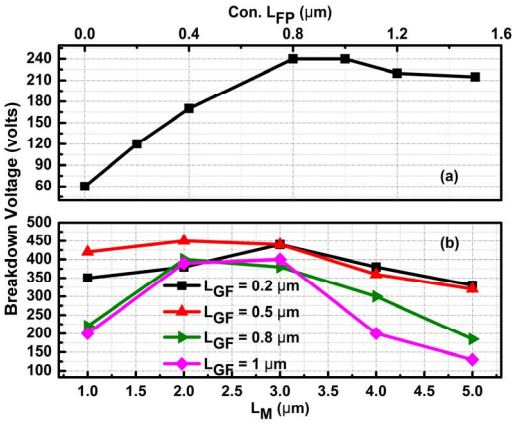

Fig.2 (a) Simulated breakdown voltage as a function of *FP* length overlap drift region L_{FP} for convention *FP HEMTs* (b) breakdown voltage as a function of L_M with different L_{GF}. All devices have the same physical dimension, where L_{GS} = 1.1µm, L_G = 0.8 µm and L_{GD} = 6 µm.

that the devices with AFP still have room to accommodate higher drain voltage and with lower gate edge electric field induced leakage. Next, conventional FP and AFP devices with the same equivalent FP dimensions and the same cell pitch were also simulated at near breakdown conditions ($E = E_c$ =

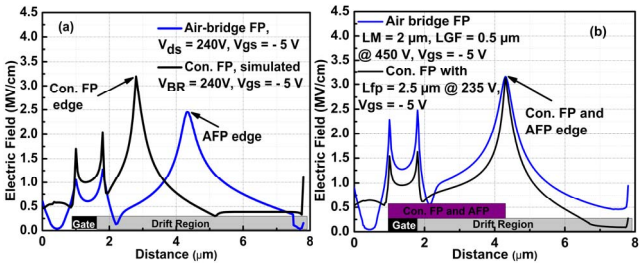

Fig.3 (a) Simulated electric field strength of a AFP device with L_M = 2 µm, L_{GF} = 0.5µm with the drain applied voltage of V_{ds} = 240 V and a conventional FP device (simulated breakdown voltage $BV_{(s)}$ = 240 V) with L_{FP} = 1.2 µm. The simulated breakdown voltage of the AFP device with L_M = 2 µm, L_{GF} = 0.5µm is 450 V. (b) Simulated electric field for devices with the same effective FP length (L_M + L_{GF} = L_{FP} = 2.5 µm). Critical electric field E_c is around 3.3 MV/cm. Acceptor and donor like traps (Density = 2×10^{16} cm^{-3}, energy level E_t = 0.9 eV) was modeled under the gate of channel area. Electron and hole ionization rates for the GaN buffer and channel regions were specified as 2.6×10^{8} cm^{-1} and 4.98×10^{6} cm^{-1}, respectively.

3.3 MV/cm). The simulated drain voltage of the HEMT with AFP having L_M = 2 µm, L_{GF} = 0.5 µm is 450 V. The simulated drain voltage for the device with conventional FP having L_{FP} = 2.5 µm is 235 V. The electric field distributions for HEMTs near breakdown with the same effective FP length are as shown in Fig. 3 (b). The low dielectric constant of air can better modulate the surface electric field distribution, allowing the device with AFP to support higher breakdown voltage even with the same device dimensions. From Fig.2 (b), it can be easily observed that breakdown voltage has the best device dimension tolerance as a function of L_M with L_{GF} = 0.5 µm. Breakdown voltage degrades slightly from 375 V for L_M = 2 µm, L_{GF} = 0.5 µm to 325 V for L_M = 5 µm, L_{GF} = 0.5 µm. The breakdown voltage degrades dramatically for those devices with L_{GF} above 0.8 µm, L_M = 5 µm. Surface electric field

distributions for those devices with L_M = 5 μm, L_{GF} length from 0.2 μm to 1 μm are as shown in Fig. 4.

From Fig. 4, it can be easily observed that surface peak electric field moves to the drain side with increasing L_{GF}.

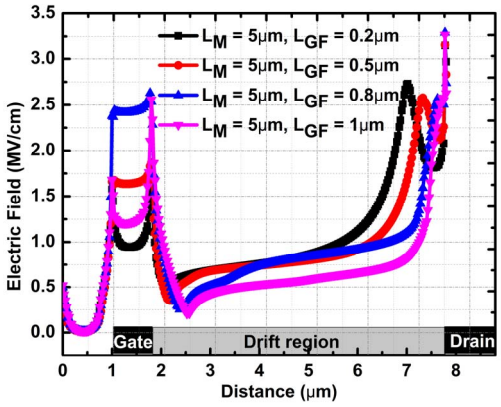

Fig.4 Simulated electric field distribution along AlGaN/GaN interface as a function of L_{GF}, where L_M = 5 μm.

Premature breakdown happens near the drain side. From Fig. 2 (b), breakdown voltage also degrades dramatically for those devices with L_M = 1 μm and, L_{GF} above 0.8 μm. Surface electric field distributions for those devices are as shown in Fig. 5 to help understand the possible reasons. As illustrated in Fig. 5,

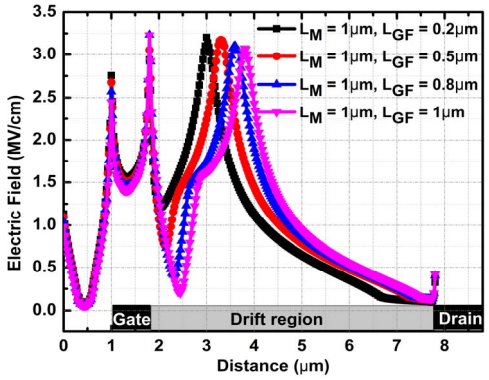

Fig.5 Simulated electric field distribution along AlGaN/GaN interface as a function of L_{GF}, where L_M = 1 μm.

electric field strength near FP edge decreases with increasing L_{GF}, while the peak electric field near the drain side gate edge increases with increasing L_{GF}. This can indicate that the premature breakdown happens near the gate edge.

IV. Experimental Results

The device active area was first defined by mesa etching. Ohmic contact using Ti/Al/Ni/Au (285 nm) was deposited by e-beam evaporation and annealed at 850 °C for 30 s in N_2 ambient. The Schottky gate was formed by an e-beam evaporated Pt-based (430 nm) layer without annealing. This was defined using lift-off processes. A 150 nm PECVD Si_3N_4 passivation film was deposited followed by a 1000 nm thick layer of Au metallization, which can be used to implement the AFP or conventional FP. Al mole fraction in the AlGaN layer

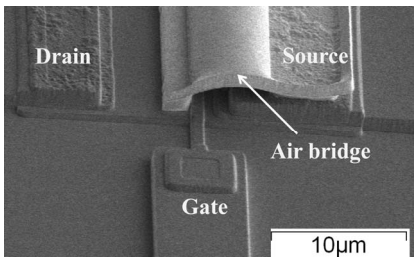

Fig.6 SEM view of fabricated novel AFP HEMT.

was 0.28. A sheet carrier density of 1.1×10^{13} cm^{-2} and an electron mobility of 1800 cm^2 V^{-1} S^{-1} were obtained by Hall measurements. Transmission Line Measurement (TLM) indicates that the ohmic contact resistance varies from 0.52 and 0.67 ohm-mm across the wafer.

Fig. 7 (a) illustrates the measured C_{gs} as a function of V_{gs}

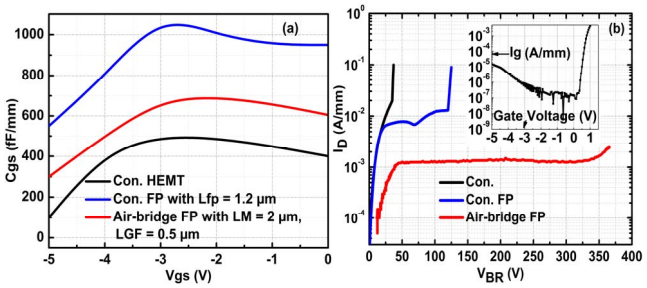

Fig.7 (a) Measured C_{gs} as a function of V_{gs}. (b) OFF-state of *I-V* characteristics of the fabricated AlGaN/GaN HEMTs. The inset shows intrinsic gate leakage current. The breakdown voltages (actual breakdown point) for devices without FP, with FP and with the proposed AFP are 37 V, 125 V, and 375 V, respectively. Unless otherwise noted, the devices have the same designed physical dimension, where L_{FP} = 1.2 μm, L_{GS} = 1.1μm, L_G = 0.8 μm, L_{GF} = 0.5 μm, L_M = 2 μm and L_{GD} = 6 μm.

for HEMTs with and without conventional FP (L_{FP} = 1.2 μm), and AFP with L_M = 2μm, L_{GF} = 0.5μm. Since the dielectric constant of air is 1, the air-bridge HEMT exhibits much lower C_{gs} when compared to the case with conventional FP. OFF-state I-V characteristics of these devices are as shown in Fig. 2

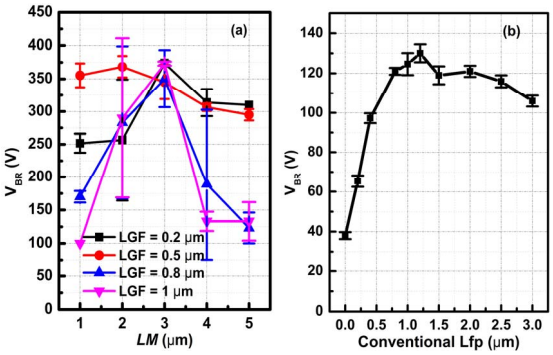

Fig.8 (a) Measured breakdown voltage (V_{BR}) as a function of L_M with different L_{GF} and (b) breakdown voltage as a function of convention L_{FP}.

(b). For the conventional HEMT without FP, a forward blocking voltage of 37 V was obtained with a drain leakage current of over 10^{-2} A/mm before breakdown occurs with V_{GS} = −5 V. The HEMT with conventional optimized FP has an

improved breakdown voltage of 125 V. The leakage current was also slightly suppressed. The proposed HEMT with AFP achieved a forward blocking voltage of 375 V, which is three times higher than the HEMT with conventional FP. Furthermore, the leakage current for the HEMT with AFP is one order of magnitude lower when compared to the conventional devices, from 10^{-2} A/mm to around 10^{-3} A/mm.

The measured breakdown voltages (V_{BR}) as a function of L_M with different L_{GF} are as shown in Fig. 8 (a). Three samples from different wafers were measured. It can be observed that the testing results of the breakdown voltage also has the best process tolerance as a function of L_M with L_{GF} = 0.5 µm when compared to the simulation results. Breakdown voltage degrades slightly from 375 V for L_M = 2 µm, L_{GF} = 0.5 µm to 325 V for L_M = 5 µm, L_{GF} = 0.5 µm. The breakdown voltage degrades dramatically for those devices with L_{GF} above 0.8 µm, L_M above 3 µm and L_{GF} above 0.8 µm, L_M below 2 µm.

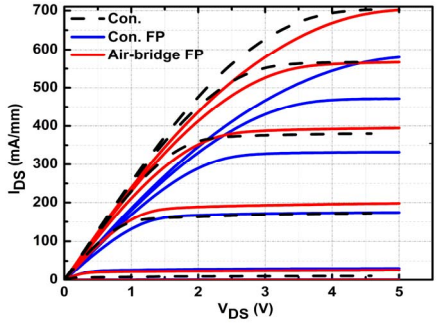

Fig.9 Measured output IV characteristics of conventional HEMT (dashed line), convention field plate HEMT (blue line) and the proposed air bridge field plate (red line) with V_{GS} from − 6 V to 0 V (step = 1 V) and V_{DS} from 0 to 5 V, where the $R_{on,sp}$ at V_{GS} = 0 V are 0.56 mΩ·cm^2, 0.79 mΩ·cm^2 and 0.58 mΩ·cm^2, respectively. The cell pitch of 13.9 µm is taken as the distance between the source and drain (including contact windows) multiplied by the finger length, was used for specific $R_{on,sp}$ calculation.

These results show good agreement with simulation results shown above. Breakdown voltage of the device with conventional FP is also shown in Fig.8 (b). The longest LFP fabricated was 3 µm. Breakdown voltage increases from 37V without FP to 125 V with conventional L_{FP} length of ~1 µm. No further increase in breakdown voltage was observed after this point.

Fig.9 shows the forward IV characteristics of the device with AFP, the conventional HEMTs with and without FP. The HEMT with conventional FP shows a large degradation of the saturation current from 700 mA/mm for conventional HEMT without FP to 550 mA/mm for the HEMT with conventional FP. $R_{on,sp}$ increases from 0.56 mΩ·cm^2 for conventional HEMT without FP to 0.79 mΩ·cm^2 with conventional FP. This phenomenon was also shown in [13]. It can be explained as the 2-DEG will be affected by the lowest potential of the metal FP with relative thin passivation layer (150 nm). The HEMT with AFP shows a much lower degradation in both $R_{on,sp}$ and the saturation current. The measured $R_{on,sp}$ of 0.58 mΩ·cm^2 represents a 37% improvement when compared to the HEMT with conventional FP.

V. Conclusion

AlGaN/GaN HEMT featuring a novel AFP has been experimentally verified. Fabrication results show good agreement with simulation results. When comparing to HEMTs with conventional FP, a 3× higher breakdown voltage was obtained. The process for the AFP HEMT is fully compatible with the commercial RF GaN technology without the need for any additional photolithography and processing step.

Acknowledgment

This work was supported in part by the China Scholarship Council (File No. 2009607040), Auto21, a Network Centre of Excellence in Canada and NSERC, Natural Science and Engineering Research Council of Canada. We would like to acknowledge National Research Council Canada and Canadian Microsystems Corp. for the provision of device fabrication and design support that facilitated this research.

References

[1] G. Xie, E. Xu, J. Lee, N. Hashemi, B. Zhang, F.Y. Fu and W.T. Ng, "Breakdown Voltage Enhancement Technique for RF Based AlGaN/GaN HEMTs with a Source-connected Air-bridge Field Plate," IEEE Electron Device Lett. (Accepted for publication, Feb. 2012).

[2] T. P. Chow, R. Tyagi. Wide bandgap compound semiconductors for superior high-voltage unipolar power devices. IEEE Trans. Electron Devices, vol. 41, no. 8, (1994) 1481–1483.

[3] J. P. Ibbetson, P. T. Fini, K. D. Ness, "Polarization effects, surface states, and the source of electrons in AlGaN/GaN heterostructure field effect transistors," App. Physic Lett. vol. 77, No. 2, July 2000.

[4] T. Nanjo, M. Takeuchi, "Remarkable breakdown voltage enhancement in AlGaN channel high electron mobility transistors,"App. Physics Lett. 92, 263502(2008).

[5] Shuming Xu, Jacek Korec, "Power LDMOS Transistor", US Patent 7235845 B2.

[6] Shuming Xu, Jacek Korec, etc,al, "NexFET A New Power Device" IEDM 2009, Baltimore, MD.

[7] Y. Ando, Y. Okamoto, H. Miyamoto, T. Nakayama, T. Inoue, and M. Kuzuhara, " 10-W/mm AlGaN-GaN HFET With a Field Modulating Plate," IEEE Electron Device Lett. 24 (2003) 289.

[8] K. S. Boutros. GaN Switching Devices for High-Frequency, KW Power Conversion", ISPSD 2006, Naples, Italy.

[9] M. L. Balzan, M. J. Drinkwine, and T. A. Winslow, "GaAs MESFET with Source-Connected Field Plate for High Voltage MMICs," CS MANTECH Conference, April 14-17, 2008, Chicago, Illinois, USA.

[10] www.crosslight.com, user's manual.

[11] A.G. Chynoweth, Phys., Rev.. vol. 109, p. 1537, 1958.

[12] I. H. Oguzman, E. Bellotti, "Theory of hole initiated impact ionization in bulk zincblende and wurtzite GaN", *J. Appl. Phys*., Vol. 81, pp. 7827-34, 1997.

[13] Wataru Saito, Yoshiharu Takada, Masahiko Kuraguchi, Kunio Tsuda, Ichiro Omura and Tsuneo Ogura, "Design and Demonstration of High Breakdown Voltage GaN High Electron Mobility Transistor (HEMT) Using Field Plate Structure for Power Electronics Application," Jpn.Journal of Applied Physics., Vol. 43, No. 4B, 2004, pp.2239-2242.